

Analysis of Transmission Line Structures Using a New Image–Mode Green's Function

I. TAI LU, MEMBER, IEEE, AND R. L. OLESEN, MEMBER, IEEE

Abstract—A hybrid image–mode–moment method is developed for the quasi-TEM analysis of transmission lines of arbitrary cross section and number suspended between infinite parallel ground planes. This new method combines the conventional moment method and a new image–mode Green's function systematically in a single formulation. The moment method is employed to model the interaction between transmission lines, and the new image-mode method is used to furnish the Green's function of the parallel plates. Several configurations are studied and are compared with work given in the references where possible.

I. INTRODUCTION

Shielded multiconductor transmission lines of arbitrary cross section embedded in multilayered dielectric media have applications in coupler and filter design. For complex structures such as these, an appropriate procedure for analysis is the moment method. However, difficulties arise with the requirement of finding an appropriate Green's function for the layered media which exhibits numerical efficiency.

Under a quasi-TEM approximation, the field of the transverse cross section is governed by two-dimensional static field equations. For solution, one must solve the Green's function problem of Poisson's equations subject to the boundary conditions. A free-space Green's function has been used for the solution of this type of problem [1]. An advantage of this approach is the simplicity of the Green's function; however, this requires the solution of a large system of simultaneous equations. Layered Green's functions can overcome these difficulties but they can be very complicated to solve. There are three conventional alternative representations of the Green's function for layered media [2]–[5].

An image representation [2] is suitable for structures which have few layers, typically one or two. This is because a proliferation of images makes this representation impractical when the number of layers is large. This representation is numerically efficient only when the source and the receiver are close to each other compared to the overall dimensions of the structure within which they are placed. A second representation [3], the spectral integral, has convergent properties similar to those of the image representation. The spectral integral formulates the Green's function in terms of a superposition of evanescent spectra, which represent all of the images collectively and, therefore, can alleviate the difficulties of the image proliferations. However, the image representation is convenient for the separation of the dominant images, which experience fewer reflections and hence have a stronger influence, from the rest of the images. This property is especially important when the source and receiver overlap each other, in which case the singular contribution due to the direct source has to be treated separately. Finally, there is

Manuscript received February 10, 1989; revised January 15, 1990. This work was supported in part by the National Science Foundation under Contract ECS-8707615 and by the Joint Services Electronics Program under Contract F49620-88-C-0075.

The authors are with the Weber Research Institute, Department of Electrical Engineering and Computer Science, Polytechnic University, Farmingdale, NY 11735.

IEEE Log Number 9034914

the modal representation [4], [5]. This option represents the Green's function in terms of evanescent modes. Higher order modes die out quickly when the source and the receiver are widely separated, but are not negligible for a small separation. The convergent properties of the modal representation complement those of the previous two representations.

Due to the complementary properties of these conventional representations for the Green's function, it may be advantageous to combine them in a single formulation which would achieve numerical efficiency for a broad class of problems. In fact, this type of hybrid approach has been developed in the dynamic case for a single slab [6] generalized to multilayered media [7] and to a cavity [8]. However, the hybrid ray–mode method is most commonly thought of as being useful for large waveguides, which support many propagating modes. Here, we extend the theory to the *static limit*, where no propagating spectra exist. By realizing that images, modes (evanescent), and spectra (evanescent) in the static case are analogous to rays, modes (evanescent and propagating), and spectra (evanescent and propagating) in the dynamic case, respectively, one can apply the methods developed previously for the dynamic problems to the static problems.

For a small separation between the source and the receiver, a modified image solution is developed to represent dominant image terms in closed form and treat the rest of the images collectively as a remainder. This remainder, represented by a spectral integral, may be evaluated by numerical integration along a fast convergent path through contour deformation in the complex spectral domain. (Unlike the dynamic case, there will be no poles intercepted by this contour deformation.) This modified image solution has the advantages of both image and spectral representations, i.e., convenience for the separation of the singular term and a remedy for the difficulty arising from image proliferations. For a large separation between the source and the receiver, the modal solution is very efficient. An image-mode formulation is developed to combine the modified image representation with the modal method to provide an efficient algorithm for all possible arrangements of source and receiver locations. The new Green's function formulation is suitable for application of the moment method to the analysis of transmission line structures.

This new image–mode–moment method is applicable not only to the above-mentioned microwave devices, but also to the much broader area of monolithic integrated circuits and printed circuits, where their general models can be described by multiple conducting (or dielectric) rods or strips embedded in layered structures. The extension of the quasi-TEM analysis to a full-wave analysis, if desirable, merely requires the replacement of the image–mode formulation by the analogous form in the dynamic case [9].

II. FORMULATION

We consider L conductors of arbitrary shapes and locations within a pair of parallel grounded conducting plates. The voltage at any point (x, z) within the parallel plates can be represented by a sum of surface integrals, which are given by

$$V(x, z) = \sum_{l=1}^L \int_{s_l} \frac{\sigma_l(x', z')}{\epsilon} G(x; z, x', z') ds_l \quad (x', z') \in s_l \quad (1)$$

where σ_l is the unknown charge density, s_l is an integration path along the boundary of the l th conductor, and ϵ is the permittivity of the medium. $G(x, z; x', z')$ is the Green's function which represents the voltage at (x, z) due to a line charge at (x', z') . By letting (x, z) represent points on the surfaces of conductors, we have a set of L simultaneous integral equations which can be solved by the moment method. After solving for σ_l , the total charge on the l th conductor and, hence, the capacitance matrix of the system can be derived. In the present paper, the Green's function in (1) is given by the image-mode method, which exhibits accelerated convergence. The numerical efficiency of the image-mode Green's function makes use of the moment method practical, even for a large system of simultaneous equations.

III. GREEN'S FUNCTION FORMULATION FOR PARALLEL PLATES

We seek the solution of the two-dimensional problem

$$\left[\frac{\partial^2}{\partial x^2} + \frac{\partial^2}{\partial z^2} \right] G(x, x'; z, z') = -\delta(x - x')\delta(z - z') \quad (2)$$

excited by a line source located at $x = x'$, $z = z'$ in a parallel-plate waveguide with walls at $z = 0$ and $z = a$ where $G = 0$. The alternative representations for the static Green's function are similar to that given in the dynamic case [6]. Note that the dynamic case has both propagating and evanescent spectra; however, the static case has only evanescent spectra.

A. Integral Representation

Following a Fourier transform and the characteristic Green's function method, we find the solution for the two-dimensional spectral Green's function to be

$$G = \int_{-\infty}^{\infty} \frac{A(\zeta)}{1 - e^{2i\lambda a}} d\zeta, \\ A(\zeta) \equiv \frac{e^{i\zeta(x-x')}}{-4\pi i \lambda} [e^{i\lambda|z-z'|} - e^{i\lambda(z+z')} - e^{i\lambda(2a-(z+z'))} + e^{i\lambda(2a-|z-z'|)}] \quad (3)$$

where $\lambda = (-\zeta^2)^{1/2}$ is defined to be positive when real and to have a positive imaginary part when complex. Although the integrand in (3) is an even function of λ , we shall require this definition for image expansions in subsequent developments. There are pole singularities ($\zeta = \pm im\pi/a$, $m = 1, 2, \dots$) contained in the integrand of (3).

B. Modal Representation

The integrand decays in the upper half of the ζ plane and the lower half of the ζ plane, for $x > x'$ and $x < x'$, respectively. By the residue theorem we have the sum of decaying modes along x away from the source plane $x = x'$:

$$G = \sum_{m=1}^{\infty} \frac{1}{\pi} \frac{1}{m} \sin\left(\frac{m\pi}{a} z\right) \sin\left(\frac{m\pi}{a} z'\right) \exp\left(-\frac{m\pi}{a} |x - x'|\right). \quad (4)$$

For large $|x - x'|$ the modal representation converges very rapidly due to the decaying exponential dependence. If, however, the source and the receiver are close, the modal representation converges very slowly, requiring many summation terms.

C. Image Representation

Expanding the denominator of (3) in a geometric series, we obtain the following image representation for the Green's function:

$$G = \sum_{\alpha=0}^{\infty} G_{\alpha}, \quad G_{\alpha} = \int_{-\infty}^{\infty} A(\zeta) e^{2i\lambda a\alpha} d\zeta. \quad (5)$$

The integral in (5) can be written in closed form:

$$G_{\alpha} = \frac{-1}{4\pi} \ln \left\{ \frac{(x - x')^2 + (2\alpha a + |z - z'|)^2}{(x - x')^2 + (2\alpha a + (z + z'))^2} \cdot \frac{(x - x')^2 + (2(\alpha + 1)a - |z - z'|)^2}{(x - x')^2 + (2(\alpha + 1)a - (z + z'))^2} \right\}. \quad (6)$$

Notice that (5) with (6) is the conventional image solution. The infinite image sum can, under certain conditions (e.g., $|x - x'| \gg a$), exhibit poor convergence. In the next section, the infinite sum is converted to a finite sum plus a remainder in order to improve the computational efficiency.

D. Modified Image Representation

Expanding the denominator of (3) in a partial geometric series, the infinite sum in (5) can be written as a finite sum plus a remainder term:

$$G = \sum_{n=N}^{N-1} G_n + R_N, \quad R_N \equiv \sum_{n=N}^{\infty} G_n = \int_{-\infty}^{\infty} \frac{A(\zeta) e^{2iN\lambda a}}{1 - e^{2i\lambda a}} d\zeta. \quad (7)$$

The direct image term is separated explicitly in (7), which behaves singularly if the source is close to the receiver. The remainder is nothing but a collection of images, which can be evaluated by a power series summation and reformulated into a closed form or can be represented as a spectral integral and integrated along the steepest decent path (see [7]). Generalization to multilayered structures is straightforward by employing the matrix formulation shown in [7]. The convergence of the numerical approach is sufficiently high to make a closed form unnecessary for multilayered structures.

E. Image-Mode Representation

For solution of problems where the separation between the source and the receiver cannot be limited so as to be useful for the image or mode representations, a mixed image-mode representation is likely to be more numerically efficient. In this case the Green's function will be reduced to the modal solution (4) when $|x - x'|$ is large and to the modified image solution (8) when $|x - x'|$ is small. The modified image solution will be further reduced to image terms alone if the remainder is negligible. During implementation we predetermine a threshold value T for $|x - x'|$ where the mode and modified image formats are employed for $T < |x - x'|$ and $T > |x - x'|$, respectively. Small perturbations of T do not affect the accuracy or efficiency of the algorithm. Thus, the determination of T is not crucial and can be done systematically. Basic rules are given in [9].

IV. NUMERICAL RESULTS

The configuration considered for the numerical analysis is shown in Fig. 1. Also considered is a single conducting rod. Parts (a) and (b) of Fig. 2 are plots of the surface charge density on the two conductors. This problem has been considered by a modal Green's function method [5]. Comparisons of this paper's

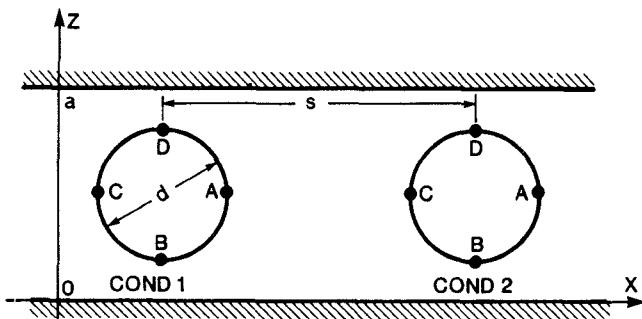
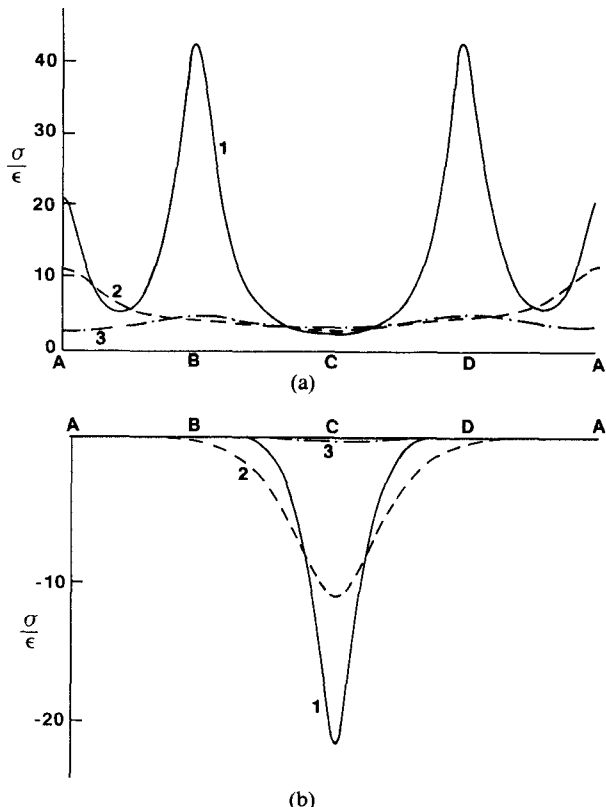


Fig. 1. The configuration considered for the numerical analysis.

Fig. 2. Surface charge densities on the two conductors of Fig. 1 versus boundary elements, denoted clockwise from point A. The voltage on the first conductor is 1 V, and the second conductor and the two conducting planes are grounded. (a) First conductor. (b) Second conductor. 1) $d/a = 0.96$, $s/a = 1.06$; 2) $d/a = 0.40$, $s/a = 0.48$; 3) $d/a = 0.544$, $s/a = 1.168$.

results with those of [5] and [10] are shown in Tables I and II; the agreement is within 2%.

V. CONCLUSIONS

It has been demonstrated that a multiconductor transmission line can be efficiently analyzed using a new method which combines the moment method with a new image-mode Green's function formulation. The image-mode method is a static extension of the hybrid ray-mode formulation, which to date has been considered desirable only for large waveguides, which support many propagating modes. Here we have shown that the concept of combining resonant solutions such as modes with "traveling" solutions such as rays is useful even in the static extreme. The moment method's advantage is its flexibility to model arbitrarily shaped, and placed, finite structures. The numerical efficiency of the image-mode Green's function makes

TABLE I
COMPARISON OF IMAGE-MODE-MOMENT METHOD SOLUTION
WITH REFERENCES FOR THE NORMALIZED CAPACITANCE
OF A SINGLE ROD

d/a	s/a	This Method		References	Remarks
		$V_1 = 1.0$ volt	$V_1 = 0.5$ volt		
0.800	2.300	7.378	7.370	[10] See Table III	
0.600	2.100	4.249	4.274	[5] See Table I	
0.400	1.900	2.730	2.744	$C/2\epsilon$	
0.200	1.700	1.707	1.716	$C/2\epsilon$	
0.100	1.600	1.242	1.230	Single Rod Approximation Used in Ref. [10]	"

TABLE II
COMPARISON OF IMAGE-MODE-MOMENT METHOD SOLUTION WITH
REFERENCES FOR THE NORMALIZED CAPACITANCE
OF A TWO-ROD CONFIGURATION

d/a	s/a	This Method		References
		$V_1 = V_2 = 1.0$ volt	$V_1 = V_2 = -1.0$ volt	
		C/ϵ	C/ϵ	[5] See Table II (Q=1)
0.354	0.530	3.912	7.543	3.913
0.400	0.480	4.167	11.240	4.165
0.400	0.520	4.265	9.558	4.263
0.400	1.160	5.217	5.700	5.213
0.544	1.712	7.388	7.535	7.386
		$V_1 = 1.0$ volt	$V_2 = -1.0$ volt	
		C/ϵ	C/ϵ	[5] See Table II (Q=-1)
0.354	0.530	7.543	7.543	7.543
0.400	0.480	11.237	11.237	11.237
0.400	0.520	9.512	9.512	9.512
0.400	1.160	5.694	5.694	5.694
0.544	1.712	7.530	7.530	7.530

use of the moment method practical in single-layer or multilayered media. This algorithm is not limited to the analysis of two conductors; any number could be considered. Iterative schemes are available to provide for efficient computation of mutual coupling. In addition the close proximity of conductors is not a problem, due to the explicit removal of any singularities encountered. The combination of the most efficient global Green's function solution (image-mode) with a flexible local coupling operator (moment method) is potentially very powerful for application to many problems with planar symmetry.

REFERENCES

- [1] C. Wie, R. F. Harrington, J. Mautz, and T. Sarkar, "Multiconductor transmission lines in multi-layered dielectric media," *IEEE Trans. Microwave Theory Tech.*, vol. MTT-32, pp. 439-449, Apr. 1984.
- [2] W. T. Weeks, "Calculation of coefficients of capacitance of multiconductor transmission lines in the presence of a dielectric interface," *IEEE Trans. Microwave Theory Tech.*, vol. MTT-18, pp. 35-43, Jan. 1970.
- [3] A. Farrar and A. T. Adams, "Multi-layer microstrip transmission lines," *IEEE Trans. Microwave Theory Tech.*, vol. MTT-22, pp. 889-891, Oct. 1974.
- [4] R. Mansour and R. Macphie, "A unified hybrid-mode analysis for planar transmission lines with multi-layer isotropic/anisotropic substrates," *IEEE Trans. Microwave Theory Tech.*, vol. MTT-35, pp. 1382-1391, Dec. 1987.
- [5] J. G. Fikioris and J. L. Tsalamengas, "Exact solutions for rectangularly shielded lines by the Carleman-Vekua Method," *IEEE Trans. Microwave Theory Tech.*, vol. 36, pp. 659-675, Apr. 1988.
- [6] L. B. Felsen and A. H. Kamel, "Hybrid ray-mode formulation of parallel plane waveguide Green's functions," *IEEE Trans. Antennas Propagat.*, vol. AP-29, pp. 637-649, July 1981.
- [7] I. T. Lu and L. B. Felsen, "Matrix Green's functions for array-type sources and receivers in multiwave layered media," *Geophys. J. Roy. Astron. Soc.*, vol. 84, pp. 31-48, 1986.

- [8] D. Wu and D. C. Chang, "A hybrid representation of the Green's function in an overmoded rectangular cavity," *IEEE Trans. Microwave Theory Tech.*, vol. 36, pp. 1334-1342, Sept. 1988.
- [9] I. T. Lu, "A Hybrid ray-mode-(boundary element method)," *J. Electromagn. Waves and Appl.*, to be published.
- [10] E. G. Crystal, "Coupled circular cylindrical rods between parallel ground planes," *IEEE Trans. Microwave Theory Tech.*, vol. MTT-12, pp. 428-439, July 1964.

The Design of an Ultra-Broad-Band 3 dB Coupler in Dielectric Waveguide

YING SHEN, DE-MING XU, AND CHEN LING

Abstract—A new structure of embedding dielectric waveguide coupler is described which offers advantages such as very flat frequency response over 50% bandwidth, simple construction, and good repeatability. A theoretical analysis by a superposition of normal modes is presented. Experimental results at the 3 mm wave band are given which show agreement with theoretical calculations.

I. INTRODUCTION

Traditional dielectric waveguide (DW) couplers are made with two identical uniform DW's (shown in Fig. 1(a)) [5], [1]. This structure has narrow bandwidth response characteristics. The reasons for this are that 1) all the power propagated in one guide can be transferred to the other if the coupling region is long enough, so that the coupling distance is strongly frequency dependent; 2) the coupling between two DW's depends on evanescent fields; and 3) both guides have the same dispersive characteristics, therefore they work with each other.

Many researchers have treated the problem of designing dielectric waveguide couplers for millimeter-wave applications [1]-[9], and certain techniques used in the very well known Riblet coupler date from 30 years ago [6]. Recently these techniques have been of interest to Kim *et al.* [3] and He [4], who improved reason 2) described above (see Fig. 1(b)). In 1987, Ikalainen and Matthaei [1] obtained wide bandwidth as well by improving reason 1); they proposed an asymmetrical cross section DW coupler (see Fig. 1(c)).

In this paper, a new kind of directional coupler, shown in Fig. 1(d), is investigated where two coupled guides with unequal cross sections are connected directly. It combines the merits of [1], [3], and [4], and the effects of dispersion are also reduced. Therefore, ultra-broad-band frequency characteristics are achieved.

We discuss the basic principles of the connected asymmetric coupler. The theoretical bandwidth is on the order of 50%. Experimental results in the frequency range 76-110 GHz are presented, and these show agreement with theoretical calculation.

II. THEORETICAL ANALYSIS

With the simplicity of the analysis, we assume that the dielectric slab waveguide directional coupler is lossless, with the analysis being confined to the parallel coupling segment only.

Manuscript received March 15, 1989; revised October 3, 1989.

The authors are with the Department of Radio Electronics, Shanghai University of Science and Technology, Shanghai, People's Republic of China.
IEEE Log Number 9034887.

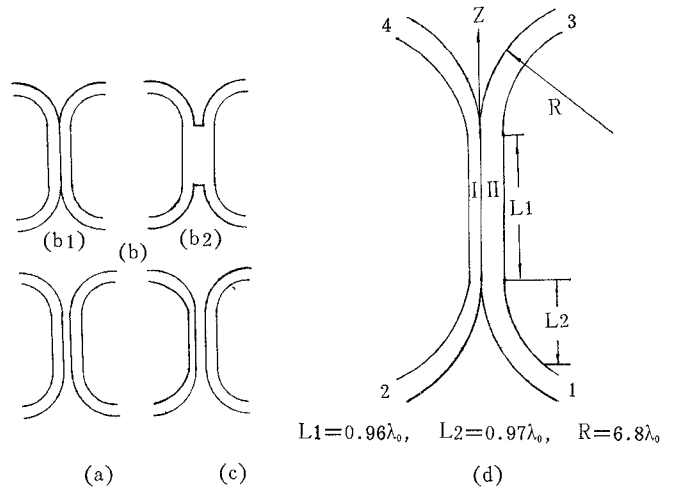
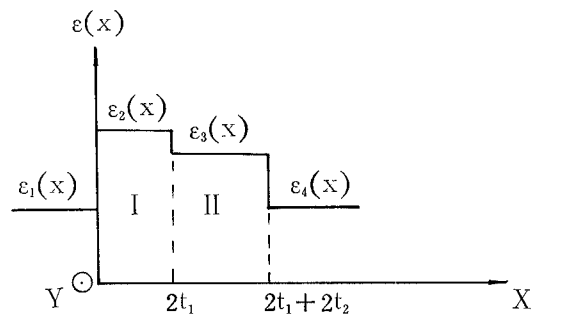


Fig. 1. Various directional couplers in dielectric waveguide.



$t_1 = 0.138\lambda_0$, $t_2 = 0.197\lambda_0$
 $\epsilon_2(x) = \epsilon_3(x) = 2.06$ teflon
 $\epsilon_1(x) = \epsilon_4(x) = 1.06$ polystyrene foam

Fig. 2. Distribution of dielectric constants.

The following theoretical analysis is based on the conditions stated above.

In Fig. 1(d) is shown the layout of the actual coupler. Let power be input into port 1; then port 4 and port 3 are the coupled and the direct port, respectively. We take the standard slab model to be a lossless dielectric medium. The dielectric constant $\epsilon(X)$ is assumed to vary only with X , as shown in Fig. 2. If the waves are assumed to travel in the Z direction with propagation constant β , then the electric and magnetic fields are independent of Y and can be expressed as

$$E = E(X) * \exp j(\omega t - \beta z)$$

$$H = H(X) * \exp j(\omega t - \beta z). \quad (1)$$

For the TE mode, it follows from Maxwell's equations that the electric field $E_Y(X)$ is described by

$$dE_Y^2(X)/dX^2 + [k^2\epsilon(X) - \beta^2]E_Y(X) = 0. \quad (2)$$